Comparison of the heat transfer capabilities of conventional single- and two-phase cooling systems for electric vehicle IGBT power module

Comparison of the heat transfer capabilities of conventional single- and two-phase cooling systems for electric vehicle IGBT power module

I. Aranzabal, I. Martinez de Alegria, N. Delmonte, P. Cova, I.Kortabarria
Universidad del País Vasco / Euskal Herriko Unibertsitatea (UPV/EHU)
University of Parma
e-mail: itxaso.aranzabal@ehu.eus, inigo.martinezdealegria@ehu.es, nicola.delmonte@unipr.it, paolo.cova@unipr.it, inigo.kortabarria@ehu.es

***Abstract*—This paper presents a comparison of conventional single-phase water/glycol liquid and innovative two-phase cooling technology for thermal management of high power electronics automotive IGBT modules during full drive cycle. The proposed two-phase cooling system is built using conventional automotive air conditioning components (condenser, expansion valve, compressor, and vapor and liquid lines) and conventional cold plate as used for single-phase cooling, thus the design does not require the development of new technology for its implementation. 3-D numerical simulation in COMSOL and experimental results of two-phase cooling have been obtained on a prototype and compared to conventional water/glycol cooling high power electronics modules, with considerable improvement on working temperature, power transfer capacity and equalization of die temperatures during a full driving cycle. These results suggest that two-phase cooling using the same cold plates as in single-phase cooling can be used to substantially improve the performance and reliability, of EV power converters without major changes.**

I. Introduction

High power density Electric Vehicle (EV) power inverters require a new approach to cope with stringent requirements of high current density, excessive ambient temperatures, humidity, vibrations, dirt in the engine compartment, reliability and cost. The heat flux of power IGBT modules for EVs is in the range of 100-150 W/cm^2 and it is projected to increase to 500 W/cm^2, as the current densities and swiching frequencies increase [1]–[3]. Development of new die technologies, such as wide bandgap (WBG), require innovative cooling methods to achieve an efficient implementation [4]. Silicon die power dissipation is close to 100 W/cm^2, while WBG dies can reach up to 1 kW/cm^2, so new efficient cooling technologies are necessary [4].

Power semiconductor devices may incur failures and lifetime reduction if the maximum junction temperature given by the manufacturer is exceeded [5], [6] and when the power cycling produces a high temperature swing [7]. Therefore, a prediction of the chip temperature in the design process is crucial for a reliable IGBT module thermal design, as well as the heat sink design, which affects the total converter size, weight and cost. The reliability of power electronic systems is also closely dependent on the thermal behavior of semiconductor devices. In [8] it is demonstrated that, for a 1.7 kV IGBT technology power inverter, increasing the cooling capacity from 50 W/cm^2 to 120 W/cm^2, the current density increases from 40 A/cm^2 to 80 A/cm^2.

Many technologies and techniques for cooling EV power modules can be found in the literature as shown in Figure 1 [1], [5], [9]–[31]. In [32] a review and classification of the main thermal management techniques is presented.

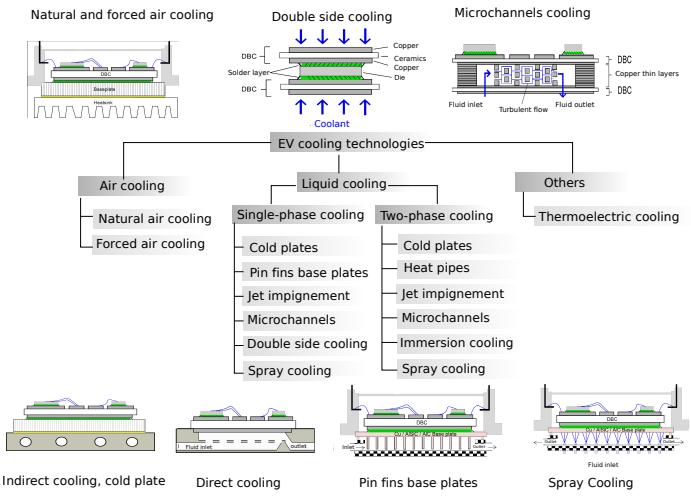

Fig. 1. Classification of EV power modules cooling technologies.

In two-phase cooling systems, the boiling effect provides the possibility of increasing heat absorption per unit volume of fluid and higher heat acquisition effectiveness (i.e., the amount of heat absorbed by a unit of flow relative to its maximum theoretical capacity). This latent heat benefit is coupled with the improved convection due to buoyancy-driven bubble formation, multi-phase turbulation, and mixing that take place within the heat transfer region. In this way, the resultant heat transfer coefficients from two-phase flow can be an order of magnitude greater than equivalent single-phase forced convection. A larger heat tranfer coefficient translates directly into a larger cooling capacity for the system [33], allowing lower flow

rates, and lower pumping power than the conventional single-phase water/glycol cold plates. In spite of these advantages, the unconventional design trade-offs in two-phase cold plates have limited the introduction of two-phase cooling in automotive power inverters.

Several papers in the scientific literature present results on two-phase cooling techniques for the removal of high heat flux. In [14], [34], authors designed a pump vaporizable dielectric fluid cooling system for power electronics systems, in [35]–[37] authors designed a two-phase microchannel heat sink capable to obtain a heat transfer coefficient up to 50000 W/m^2K. In [38], thermal simulation is used to study the effect of convective heat transfer coefficient, cold plate dimensions and total power dissipated by IGBTs on the thermal performance of the power module.

A few authors present a two-phase cooling system based on conventional A/C components. The Oak Ridge National Laboratory designed a two-phase cooling floating loop based on the EV passenger compartment A/C refrigerant system [39], [40]. In [41] a passive two-phase cooling has been designed for automotive power electronics. In [42] a device-level analytical modelling and system-level thermal simulation is used to examine and compare single-phase and two-phase cold plates for an inverter module. However, no direct experimental data is available for comparison of single-phase and two-phase cooling of EV power inverter working through the same full drive cycle, in order to assess both systems.

This paper is focused on improving the reliability of EV power converters using a two-phase cooling system with a cold plate and R134-a coolant. R134-a is already available in automotive Air Conditioning (A/C) system, it is environmentally friendly and has good heat transfer and dielectric properties [14], [43], [44].

The main goal of this work is to test and compare an experimental VCTPL (Vapour Compression Two-Phase Loop) prototype built using conventional automotive air conditioning components (condenser, expansion valve, compressor, and vapour and liquid lines) with a conventional single-phase cooling system under the same drive cycle.

Because the heat transfer coefficient, h, is not a parameter provided by manufacturers of cold plates for conventional single-phase cooling, it is necessary to determine experimentally the value of h for a specific cold plate (NHC-152), before detailed three-dimensional FEM (Finite Element Method) simulation of the two-phase cooling of IGBTs in the motor inverter could be done. Two-phase and single-phase cooling on the same cold plate have been numerically compared with multiphysics simulations to address the advantages of the first solution from the point of view of conversion efficiency and system reliability.

The following sections are presented:

- a experimental determination of the heat transfer coefficient, h, of the NHC-152 cold plate for SKIM power modules;
- the experimental results of single and two-phase cooling under a full drive cycle;
- a 3-D thermal simulation under steady state conditions of single-phase and two-phase cooling using the same cold plate.

II. Experimental characterization

By thermal characterization of the cold plate operating in single and two-phase modes, it has been possible to evaluate the thermal resistance and heat transfer coefficient of the module operating at different conditions.

Before the cold plate characterization results are presented, the test benches will be discussed.

A. Two-phase cooling system experimental platform description

A VCTPL technology has been developed, based on the conventional vapour compression refrigeration technique. The prototype consists of:

- an evaporator (the power module cold plate is incorporated as evaporator in VCTPL);
- a condenser, to transfer the heat load to ambient air;
- a compressor designed to use with dielectric fluids;
- an electronic expansion valve;
- ancillary components, for system design specifications, which include a filter, pressure transducers, manometers and thermocouples.

A schematic diagram of a VCTPL is shown in Figure 2(a), illustrating its different parts and the fluid direction inside it. Figure 2(b) shows a picture of the experimental platform.

Under steady-state conditions, when the heat released from the power module is transferred to the cold plate, the liquid starts to vaporize (R134-a refrigerant vaporizes at a low T_{sat} temperature), and absorbs heat from the power module. In the test bench of Figure 2(b), to easily generate a controlled heat, three power resistors in series have been used, instead of a semiconductor power module [1].

The vapour passes through the compressor, where it is brought to high pressure, at a temperature typically 10 °C to 15 °C higher than ambient. This hot vapour is converted to liquid in the condensing heat exchanger, where heat is transferred to the ambient air. The hot liquid refrigerant then exits the condenser and passes through an expansion valve, dropping the refrigerant to a low pressure and temperature. The low-temperature, low-pressure liquid refrigerant then enters the evaporator and the cycle begins again.

An electronic valve and a PI controller are used to ensure that the compressor is always fed with superheated gas and it is not damaged. In order to ensure that the Critical heat Flux, where bubbles are too big and dry out may occur, is not reached, the system is monitored in order to detect very sudden temperature raises. However, during tests Critical heat Flux was never reached.

[1] In order to reduce the heat transferred to the air, and ensure that the dissipated power is equal heat absorbed by the cold plate, the evaporator system has been thermally isolated by styrofoam material.

Vapour compression systems take advantage of the liquid latent heat vaporization that has a boiling point lower than the desired temperature to be managed.

B. Single-phase cooling system description

In order to provide a baseline for comparison, performance of the power inverter module with single-phase convective cooling has been included. In this way, for the single-phase cooling a water/glycol LCS-W2x420PRO liquid cooling system has been used (Figure 2(c)). The main elements are:

- two pumps to circulate the water in the closed cooling loop;
- 36 Air fans: to transfer the heat to the air;
- fans speed controller: the controller regulate the fans speed depending of the fluid outlet temperature;
- ancillary components, for system design specifications, which include a filter, thermocouples, a flow meter and pump regulators.

The low temperature water/glycol flow generated by the recirculating pump, goes to the cold plate, which absorbs the heat generated by the power module mounted on it. The hot liquid at the outlet of the cold plate is cooled by 36 fans located along the cooling loop and the heat is transferred to ambient air. Fans speed is controlled as a function of the fluid outlet temperature.

C. Experimental determination of cold plate heat transfer coefficient, h

To characterize the cold plate and evaluate its performance, it is necessary to analyse the value of the thermal resistance $R_{(s-f)}$. In a first approximation, in order to emulate the thermal pattern of a high density power module, following the procedure described in [45], the cold plate is heated by Joule effect using three series connected 22 Ω- 300 W power resistors, with capacity to dissipate up to a maximum power of 900 W. For steady state conditions the temperatures measured on the cold plate have variations less than a tenth of a degree over a period of about twenty minutes.

The manufacturer of NHC-152 cold plate provides a nominal thermal resistance, $R_{th(s-f)}$, of 0.016 K/W for single-phase liquid cooling. However, for two-phase cooling system, due to the simultaneous existence of the two-phases and possible thermal transport by convection and boiling, predicting this value is very challenging. In order to obtain accurate numerical models, a correct value of h is necessary.

When the thermophysical properties (i.e., vapor quality, pressure inside the cold plate, flow rate, etc.) in the evaporation process are unknown, based on previous studies [37], [46]–[48], the expression used to determine the average heat transfer coefficient h is the following:

$$h = \frac{1}{R_{(w-f)} \cdot A}, \tag{1}$$

$$R_{(w-f)} = R_{(s-f)} - R_{(s-w)}, \tag{2}$$

TABLE I
COLD PLATE CHARACTERIZATION FOR SINGLE-PHASE AND TWO-PHASE COOLING TECHNOLOGY.

Pd (W)	**Technology**	T_f (ºC)	Ts_{avg} (ºC)	**h** (W/m^2K)	R_{s-f} (K/W)
340	Single-phase	25.5	31.2	1362	0.016
340	Two-phase	-11.25	-6.5	1581	0.015
460	Single-phase	25.5	33.25	1344	0.016
460	Two-phase	-9	-3.2	1958	0.013
600	Single-phase	25.5	34.25	1535	0.015
600	Two-phase	-6.7	0.15	2213	0.011
760	Single-phase	27	37.05	1730	0.013
760	Two-phase	-6.65	0.9	2517	0.009
945	Single-phase	27	39.5	1862	0.013
945	Two-phase	-6.65	1.49	2953	0.008

$$R_{(s-f)} = \frac{Ts_{avg} - T_f}{P_d}, \tag{3}$$

$$T_f = \frac{T_{out} + T_{in}}{2}, \tag{4}$$

$$R_{(s-w)} = \frac{d_m}{\lambda \cdot A}, \tag{5}$$

where $R_{(w-f)}$ is the thermal resistance from the cold plate internal channel wall to the fluid, $R_{(s-f)}$ is the total thermal resistance from the cold plate to the fluid, $R_{(s-w)}$ is the thermal resistance from the cold plate top surface to the internal channel wall obtained by conduction, Ts_{avg} is the average temperature of the cold plate surface [2], T_f is the average fluid temperature, T_{in} is the saturation temperature of the refrigerant in the test section, which is measured by a temperature probe located at the inlet of the evaporator, T_{out} is the overheating saturation temperature of the refrigerant in the test section, which is measured by a temperature probe located at the outlet of the evaporator, λ is the cold plate material thermal conductivity, d_m is the distance from the cold plate top surface to the internal channel wall, P_d is the power dissipated in the module (or the total heat absorbed by the cold plate) and A is the cold plate top surface heat transfer area. Figure 3 shows the physical meaning of all the terms.

Table I presents $R_{(s-f)}$ for single-phase cooling, and h and $R_{(s-f)}$ for two-phase cooling.

These experimental results are in accordance with data provided by cold plate's manufacturer. The results demonstrate that a R134a-cooled two-phase cooling system at a flow rate of 0.2 l/min can reach values for the heat transfer coefficient and thermal resistance around 1500 W/m^2K and 3000 W/m^2K, and 0.008 K/W and 0.015 K/W respectively.

The results demonstrate that for the R134a-cooled two-phase cooling system, when heat flux is increased, the flow boiling

[2] Ts_{avg} was directly measured by thermocouples placed on the cold plate surface and contrasted by thermograms taken by an IR camera FLIR SC 430.

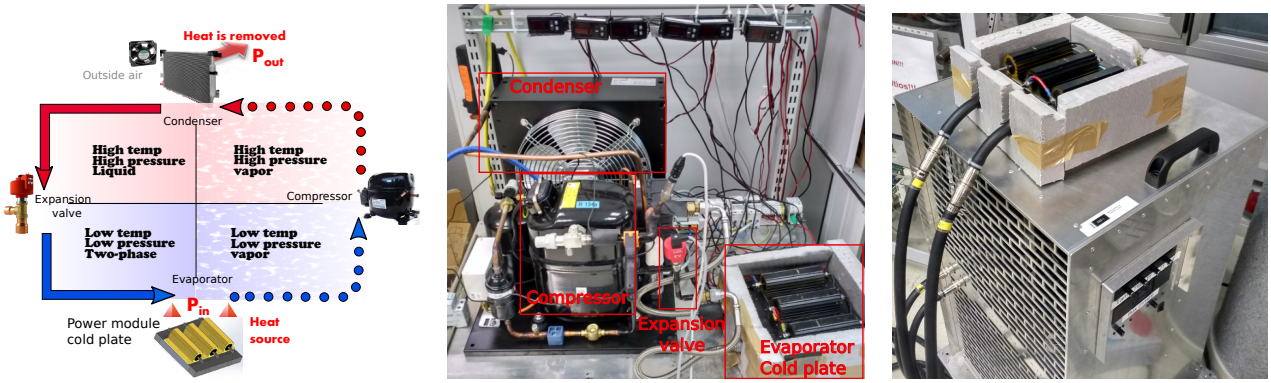

(a) Schematic diagram of the experimental vapour compression loop.

(b) Experimental vapour compression loop.

(c) Experimental water/glycol cooling system.

Fig. 2. Developed experimental platforms of EV power modules cooling systems.

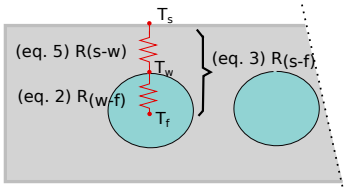

Fig. 3. Thermal resistance network of the cold plate.

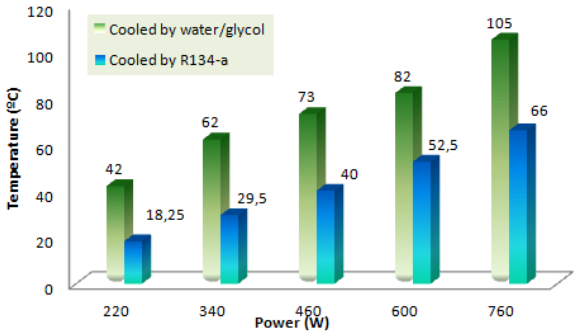

Fig. 4. Resistor surface maximum temperature operating in a two-phase and single-phase cooling modes.

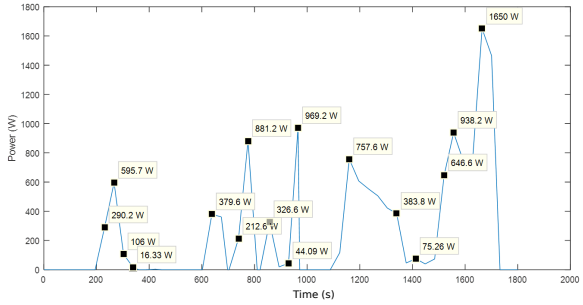

(a) Loss vs time curve derived from a WLTP driving cycle.

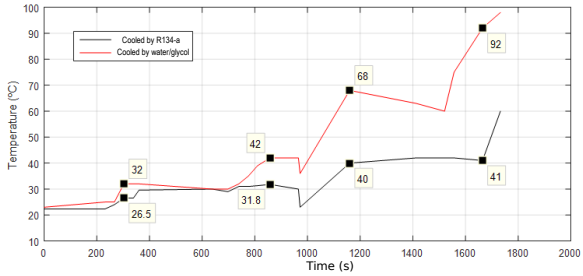

(b) Maximum resistor top surface temperature.

Fig. 5. Maximum resistor surface temperature obtained experimentally when a WLTP driving cycle is applied to the load.

heat transfer coefficient increased, which is an indication of nucleate boiling regime [49].

Figure 4 shows the average temperature measured on the resistor top surface for different dissipate powers operating in a two-phase and single-phase cooling modes.

III. WLTP DRIVING CYCLE THERMAL RESPONSE

In this section a comparison of single and two-phase cooling when a WLTP (Worldwide harmonized Light vehicles Test Procedure) driving cycle is applied to the load is shown. Additionally, to test the performance of the cooling system under close to real EV drive operation conditions, a loss vs time curve (Figure 5(a)) derived from a WLTP driving cycle [50] has been applied to the load. Driving cycles are standardized series of points, determined by governments or organizations, that represent the speed profile of a given vehicle vs time [51]. The target of driving cycles is to estimate the CO_2 emissions, energy consumption and autonomy of the vehicles. Torque, mechanical power and power losses depend on the drive and vehicle characteristics. In this particular case, inverter losses have been estimated considering a 64 kW drive of a $B-segment$ electric vehicle.

The results of the experiment demonstrate that for a R134a-cooled two-phase cooling system the maximum resistor top sur-

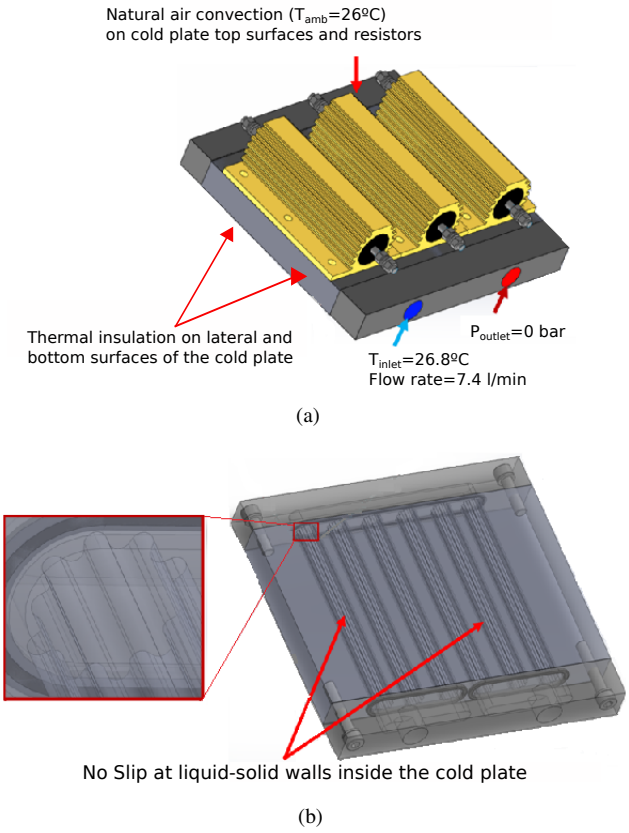

Fig. 6. a) 3D geometry of the single-phase numerical model with external boundary conditions of the thermal-fluid dynamic problem; b) 3D geometry of the cold plate with inner boundary conditions for CFD.

face temperatures are kept below the temperatures obtained in a water/glycol cooled system under same operation conditions. Therefore, two-phase cooling offers the possibility to run the module at higher current density and realize the same power level with fewer devices and smaller/lighter weight packaging, resulting in significant potential cost savings.

IV. Numerical Modeling

This section describes 3-D simulations using COMSOL Multiphysics of single and two-phase cooling using an NHC-152 cold plate for a SKIM909GD066 inverter.

A. Geometry and boundary conditions for 3-D simulation

Figure 6(a) shows the 3D geometry of the cold plate with the power resistors used during the experimental characterization with the boundary conditions set in the numerical model. The dissipated power is distributed uniformly along the wounded resistance. The cold plate shown in Figure 6(b), is composed by two 3-columns thermosiphons in series. The columns section is circular with fins.

With COMSOL Multiphysics, while a fully coupled thermal-fluid dynamic single-phase problem can be modelled with no particular troubles, the same problem with the two-phase cooling cannot be easily set. The main problem in the last case is to couple the heat transfer in solids with the evaporation of the coolant in the cold plate.

The experimental characterization described in Section II has been made to:

- validate the thermal-fluid dynamic models of the single-phase cooling;
- evaluate the thermal resistance of the cold plate when used for the two-phase cooling, in order to avoid the simulation of the evaporation, which requires a complex model with two-phase change (liquid to gas) and vapor saturation.

Simulation of the complex two-phase phenomenon, with thermal transport by boiling and convection, has been simplified with good matching between simulation and experimental results by substitution of all the mechanisms by a simple uniform heat transfer coefficient, h, along the inner walls of the cold plate.

B. Single-phase modelling validation

The water-propylene glycol 40% mixture, with a no slip boundary condition (the fluid will have zero velocity relative to the boundary) at the surfaces in contact with the aluminium cold plate channel wall has been set as coolant.

Steady state simulations for different dissipated power levels in the resistors have been obtained and compared with experimental results using thermogram images obtained using a FLIR SC 430 thermal camera.

The matching between simulations and experimental is good as can be seen comparing the thermal maps shown in Figure 7(a).

In this model, the uncertainty arise mainly by the Thermal Contact Resistance (TCR) between the resistors an the cold plate, because this parts are not clamped with well know strength. Thus, even if the thermal resistance of the Silpad used as thermal filler is known, the TCR set in the model was used as fitting parameter.

C. Two-phase modelling validation

As stated above for this case, the two-phase fluid mechanics and heat transfer details were simplified using the estimated heat transfer coefficient, h, at the inner walls, and setting a constant border condition all along the walls of the inner tubes of the cold plate. Figure 7(b) shows the thermal maps obtained by simulation and measurement in the case of P_d = 700 W, h = 2600 W/m^2K and T_{sat} = -8°C.

The large difference observed in the temperature values and in temperature distribution (Figures 7(a) and 7(b)) is due to the different physics governing both cooling solutions, where the capacity of heat absorption through phase change is much higher than through single-phase convection.

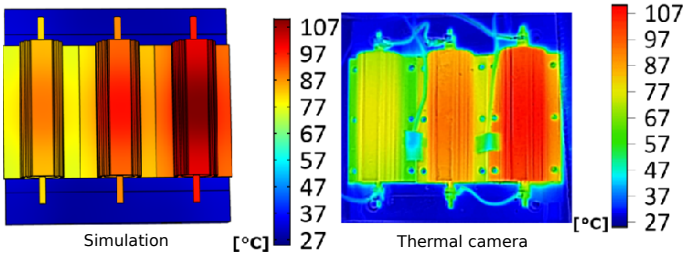

(a) P_d of 700 W, flow rate = 7.4 l/min, T_{inlet} = 27°C, T_{amb} = 26°C

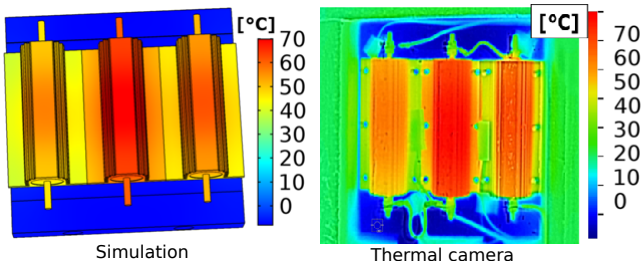

(b) P_d of 700 W, flow rate = 0.2 l/min, T_{sat} = -8°C.

Fig. 7. Thermal maps resulting by a simulation at steady state with a total dissipated power of 700 W: (a)Single-phase cooling; (b) Two-phase cooling.

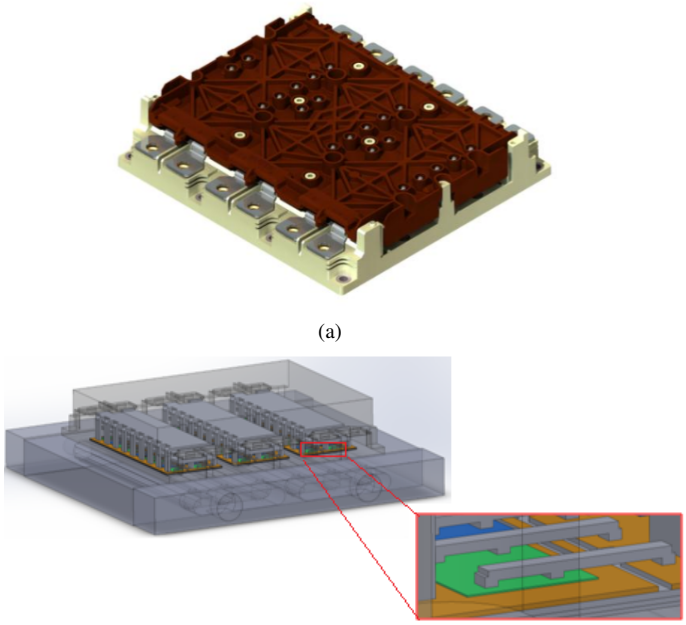

(a)

(b)

Fig. 8. a) SKIM909GD066 power module: view of the package; b) Transparency of the SKIM909GD066 module mounted on the cold plate adopted in this work. The zoomed-up inset shows how the thermal bridges are modeled by replacing the bonding wires.

D. Numerical analysis with a SKIM909GD066 power module

The SKIM909GD066 module have been specially designed for automotive applications with high power densities and harsh environmental condition operation capabilities [52]. The package and the layout at the silicon devices level are shown in Figure 8(a). Table II shows the thermal properties of each layer.

The main goal of this section is to present the comparison of die temperatures in the SKIM module between both single-phase and two-phase cooling techniques.

Device temperature depends on the internal package thermal resistance, which is introduced in COMSOL using an accurate model with detailed 3D geometry of all the layers of the SKIM module and thermal resistance of the cooler. The thermal resistance of the cooler for single-phase and two-phase cooling are those obtained in the previous sections, based on the experimentally obtained heat transfer coeficient, h. The uncertainty on the simulation results is reduced to acceptable levels, with an estimated maximum error of around $\pm$ % 5 [45].

This methodology simplifies the simulation process avoiding the time consuming cosimulation of heat transfer and fluid dynamics modules in COMSOL. After a valid equivalent heat transfer coefficient, h, has been obtained for the two phase cooled cold plate, only COMSOL heat transfer module is necessary in order to compare solutions, and to evaluate the heat spreading and thermal cross-talk among IGBTs and diodes of the power model, and in turn to evaluate the temperature of the silicon devices of the module.

The cold plate has been modeled as done for the cases described in sub-sections IV-B and IV-C. In order to keep the degrees of freedom as low as possible, the geometry of the module has been simplified as shown in Figure 8(b), drawing the top cover flat and replacing the bonding wires with geometrically simpler equivalent thermal bridges. After performing distinct simulations to observe the effect of the thermal gel (commonly used to fill the space between the plastic top cover and the power modules), it has been concluded that the utilization of thermal gel barely affects the results because almost all the heat flows towards the cold plate. Thus, to further simplify the model, the power modules were considered as encapsulated in a homogeneous plastic top cover. The simulations were carried out to solve steady-state operating conditions, setting the power dissipated by each IGBT and diode of the power module, considering the heat generated by a diode the half of the one generated by an IGBT. The simulation

TABLE II
IGBT POWER MODULE PACKAGE MATERIAL PROPERTIES.

Sheet	**Materials**	**Thickness** mm	**Ther. conduct.** $W/m \cdot K$	**Spec. heat** $J/kg \cdot K$	**Density** kg/m^3
IGBT chip	Silicon	0.15	130	700	2329
FWD chip	Silicon	0.24	130	700	2329
Die-attach	Ag sinter	0.02	250	230	7350
DBC copper 1	Copper	0.30	400	385	8960
Ceramic	Al_2O_3	0.38	35	730	3965
DBC copper 2	Copper	0.30	400	385	8960
TIM	TIM	0.25	2	1000	2900

results are shown in the next section.

V. Results and Discussion

This section analyzes the results obtained in the FEM simulations using two different approaches: single-phase cooling, using water as coolant, and two-phase cooling, using R-134a as coolant.

A. Comparison of two-phase and single-phase results

By the FEM analysis it was found that an R134a-cooled two-phase cold plate can achieve much lower device junction temperature at much lower mass flow rate than a water-cooled single-phase cold plate. In this sense, thermal simulations of the power inverter show that two-phase cooling can provide much better IGBT cooling performance at lower flow rate (see tables III and IV, where the IGBTs were numbered as shown in Figure 9(a)). For example, in the case of a dissipated power of 2106 W, with an R134a-cooled two-phase cold plate, the maximum IGBT temperature can be maintained below 62 ^oC, with T_{sat} = -8 ^oC and a flow rate of 0.2 l/min, whereas with a water single-phase cold plate, it would reach around 100 ^oC with a flow rate of 6 l/min and T_{in} = 20 ^oC. With low flow rates (less than 1 l/min as in the two-phase system), the IGBTs temperature goes above its maximum allowable junction temperature (175 ^oC).

The maximum IGBT junction temperature as a function of the power module position is given in Figure 10. It can be stated that, two-phase cooling can achieve much lower IGBT temperatures than single-phase cooling and, moreover, two-phase cooling shows an almost constant heat exchange efficiency even at very low flow rates, where single-phase cooling becomes ineffective. The simulation of the single-phase technique with P_d = 2.1 kW, T_{in}=20 ^oC and flow rate = 1 l/min, gives a $T_{max} \cong$ 150 ^oC and a temperature increase of the water close to 33 ^oC. Then, even if the maximum temperature of power devices is below the maximum allowed, the high temperature increase would imply to adopt an expensive chiller. With higher flow rates, 6 l/min or more, the temperature increase can be kept at the order of magnitude of few degrees. For a closed loop liquid cooling system, this allows the adoption of a simple radiator with fans to cool the water-glycol mixture at the desired temperature at the cold plate inlet.

For a dissipated power of 2106 W, single-phase cooling will produce a maximum gradient temperature of around 16 ^oC with 6 l/min and T_{inlet} = 20 ^oC among the IGBTs, while two-phase cooling can reduce it to around 10 ^oC , with T_{sat} = -8 ^oC and a flow rate of 0.2 l/min. Since the power conversion efficiency of the power electronic systems is determined also by the IGBT junction temperature and an uniform temperature among the IGBTs is highly desirable, it is obvious that two-phase cooling can improve the performance of the inverter from the point view of both conversion efficiency and system reliability. Further comparison between single-phase and two-phase coolers can be done observing the results in Figure 9, which shows the temperature distribution on the inverter module with water (Figure 9(c)) and R134-a (Figure 9(b)) as coolants. The large difference in the temperature values and distribution is due to the different physics governing these cooling solutions.

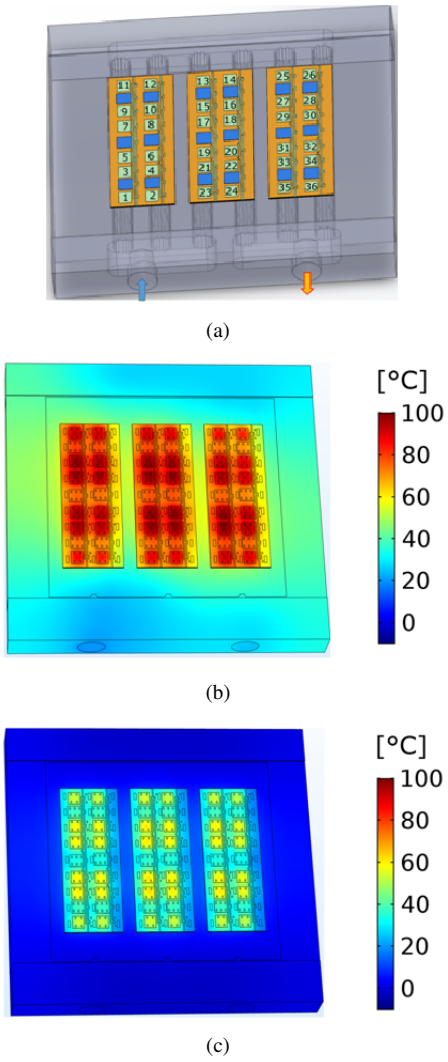

Fig. 9. Simulated temperature distribution at the silicon power device layer with P_d= 2.1 kW: a)Diodes (in blue) and IGBTs (in green) layout inside the SKIM909GD066 power module, showing how were numbered the IGBTs; b) single-phase cooling with flow rate = 6 l/min and T_{in}=20 ^oC; c) two-phase cooling with T_{sat}=-8 ^oC and flow rate=0.2 l/min.

VI. Conclusion

A comparison of two-phase cooling with single-phase cooling has been done in order to address the advantages of the two-phase solution. In this way, a VCTPL technology has been demonstrated through a series of tests using a small-scale prototype. Then, a 3-D FEM based thermal model has been designed to simulate two-phase cooling of IGBTs at the motor inverter.

The key conclusion of this study are the following:

TABLE III

SIMULATED SKIM909GD066 IGBTS MAXIMUM JUNCTION TEMPERATURES (IN ^{o}C) USING A R134-A TWO-PHASE COOLING SYSTEM WITH TSAT = -8 ^{o}C, FLOW RATE = 0.2 l/min, AND PD = 2106 W (52 W/IGBT, 13 W/DIODE).

IGBT1	IGBT1	IGBT2	IGBT3	IGBT4	IGBT5	IGBT6	IGBT7	IGBT8	IGBT9	IGBT10	IGBT11	IGBT12	IGBT13	IGBT14	IGBT15	IGBT16	IGBT17	IGBT18
	53.8	52.9	60.1	59.2	59.9	59	58.8	58.4	59.5	58.4	54.1	53.2	55	53.5	60.7	59.4	60.5	59.2
IGBT	IGBT19	IGBT20	IGBT21	IGBT22	IGBT23	IGBT24	IGBT25	IGBT26	IGBT27	IGBT28	IGBT29	IGBT30(	IGBT31	IGBT32	IGBT33	IGBT34	IGBT35	IGBT36
	61.4	59.7	61.5	60	54.8	53.3	54	51.8	59.9	57.1	59.6	57	60.5	57.2	60.6	57.8	53.8	51.8

TABLE IV

SIMULATED SKIM909GD066 IGBTS MAXIMUM JUNCTION TEMPERATURES (IN ^{o}C) USING A WATER-GLYCOL SINGLE-PHASE COOLING SYSTEM WITH TIN = 20 ^{o}C, PD = 2106 W (52 W/IGBT, 13 W/DIODE), AND DIFFERENT FLOW RATES.

Flow rate	IGBT1	IGBT2	IGBT3	IGBT4	IGBT5	IGBT6	IGBT7	IGBT8	IGBT9	IGBT10	IGBT11	IGBT12	IGBT13	IGBT14	IGBT15	IGBT16	IGBT17	IGBT18
6 (l/min)	87.2	84.9	97.3	95.6	98.1	96.5	98.8	98.1	99.9	98.3	94.6	93.1	92.8	90.8	100.5	99.7	100.7	100.3
8 (l/min)	73.6	71.3	78.8	77.1	79.2	76.5	79.3	78	81	79.2	78.2	75.6	79	78.2	82.3	83.8	80.8	83.1
10 (l/min)	72.2	70.0	77.1	75.4	77.6	74.7	77.4	75.8	79.2	77.1	76.4	73.6	77.0	76.3	80.3	81.7	78.6	81.0
12 (l/min)	71.2	69.0	75.9	74.2	76.1	73.0	76.0	74.3	77.7	75.5	75.1	72.0	75.7	74.9	78.5	80.1	77.0	79.2
Flow rate	**IGBT19**	**IGBT20**	**IGBT21**	**IGBT22**	**IGBT23**	**IGBT24**	**IGBT25**	**IGBT26**	**IGBT27**	**IGBT28**	**IGBT29**	**IGBT30**	**IGBT31**	**IGBT32**	**IGBT33**	**IGBT34**	**IGBT35**	**IGBT36**
6 l/min	100.4	100.6	99.3	99.9	89.0	90.7	87.0	83.8	96.1	92.0	97.6	93.6	99.6	96.0	100.6	97.0	93.7	91.0
8 l/min	80.7	82.6	79.8	83	74.5	77.3	74.1	71.8	78.4	76.9	77.2	76.6	79.2	77.9	80.4	80	77.3	76.4
10 l/min	78.4	80.3	77.7	80.9	72.9	75.5	72.9	70.2	76.7	75.2	74.7	74.5	77.1	75.8	77.7	77.9	75.1	74.3
12 l/min	76.7	78.7	76.3	79.5	71.6	74.2	71.6	69.1	75.2	73.8	73.5	73.2	75.6	74.4	76.1	76.4	73.8	73.0

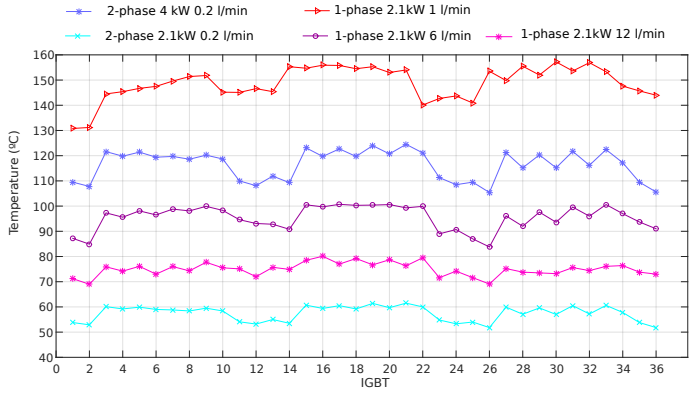

Fig. 10. SKIM909GD066 maximum IGBTs simulated temperatures at the following operating conditions: i) single-phase cooling with Pd = 2.1 kW, and Tin = 20 ^{o}C and different flow rates; ii) two-phase cooling with Tsat=-8 ^{o}C and flow rate = 0.2 l/min, for total dissipated powers of 2.1 and 4 kW.

- Simulation of the complex two-phase phenomenon, with thermal transport by boiling and convection, can be simplified with good matching between simulation and experimental results by substitution of all the mechanisms by a simple uniform heat transfer coefficient, h, along the inner walls of the cold plate.
- Simulation and experimental results show that two-phase cooling increases the heat transfer coefficient of a conventional cold plate.
- For these h values the two-phase FEM simulation shows that the maximum IGBT junction temperature can be maintained below 62 ^{o}C whereas with a water cooled system it reaches 101 ^{o}C under same operation conditions.
- FEM simulations show that the cooling capacity of the two-phase cooling system can be increased from 2.1 to 4 kW maintaining the IGBT junction temperature below 130 ^{o}C.
- Two-phase cooling provides a more even temperature distribution among the IGBTs in the power module. For a dissipated power of 2106 W, single-phase cooling will produce a maximum gradient temperature of 16 ^{o}C among the IGBTs, while two-phase cooling can reduce it to 10 ^{o}C.
- Two-phase cooling offers the possibility to run the module at higher current density and realizes the same power level with fewer devices and smaller/lighter weight packaging, resulting in significant potential cost savings.
- When compared with competing cooling technologies based on passive two-phase cooling, such as flow boiling in microchannels, jet impingement, and spray cooling, this is the only one capable of lowering the junction temperature to values below the ambient temperature. A vapor compression two-phase thermal management system may be appropriate for designing power inverters used in applications where sub-ambient temperatures are required.
- The results of the experiments demonstrate that conventional automotive A/C system can be used for a more efficient cooling of power converters.

VII. ACKNOWLEDGEMENT

This work has been carried out inside de Research and Education Unit UFI11/16 of the UPV/EHU and supported by the Department of Education, Linguistic Policy and Culture of the Basque Government within the fund for research groups of the Basque university system IT978-16, by the Ministerio de Economía y Competitividad of Spain within the project DPI2014-53685-C2-2-R and FEDER funds al also by the Government of the Basque Country within the research program ELKARTEK as the project KT4TRANS (KK-2015/00047 and KK-2016/00061).

REFERENCES

[1] A. Bhunia, S. Chandrasekaran, and C.-L. Chen, "Performance improvement of a power conversion module by liquid micro-jet impingement cooling," *IEEE Transactions on Components and Packaging Technologies*, vol. 30, pp. 309–316, 2007.

[2] I. Mudawar, D. Bharathan, K. Kelly, and S. Narumanchi, "Two-phase spray cooling of hybrid vehicle electronics," in *Proc. of Intersociety Conference onThermal and Thermomechanical Phenomena in Electronic Systems (ITHERM)*, 2008, pp. 1210–1221.

[3] T. Kanata, K. Nishiwaki, and K. Hamada, "Development trends of power semiconductors for hybrid vehicles," in *Proc. of International Power Electronics Conference (IPEC)*, 2010, pp. 778–782.

[4] A. Bar-Cohen and J. J. Albrecht, J. D.and Maurer, "Near-junction thermal management for wide bandgap devices," in *Proc. of IEEE Compound Semiconductor Integrated Circuit Symposium (CSICS)*, Oct 2011, pp. 1–5.

[5] S. Anandan and V. Ramalingam, "Thermal management of electronics: A review of literature," *Thermal Science*, vol. 12, p. 26, 2008.

[6] U. M. Choi, F. Blaabjerg, and K. B. Lee, "Study and handling methods of power igbt module failures in power electronic converter systems," *IEEE Transactions on Power Electronics*, vol. 30, pp. 2517–2533, 2015.

[7] R. Amro, J. Lutz, and A. Lindemann, "Power cycling with high temperature swing of discrete components based on different technologies," in *Proc. of IEEE 35th Annual Power Electronics Specialists Conference*, vol. 4, 2004, pp. 2593–2598 Vol.4.

[8] L. Meysenc, M. Jylhakallio, and P. Barbosa, "Power electronics cooling effectiveness versus thermal inertia," *IEEE Transactions on Power Electronics*, vol. 20, pp. 687–693, 2005.

[9] A. Bar-Cohen, R. Bahadur, and M. Iyengar, "Least-energy optimization of air-cooled heat sinks for sustainability-theory, geometry and material selection," *Energy*, vol. 31, pp. 579 – 619, 2006.

[10] P. Rodgers and V. Eveloy, "Air cooled heat sink design optimization in free convection," in *Proc. of Semiconductor Thermal Measurement and Management Symposium (SEMI-THERM)*, 2013, pp. 170–172.

[11] A. Wintrich, U. Nicolai, W. Tursky, and T. Reimann, *Application Manual Power Semiconductor*, Semicron, Ed. Semikron International GmbH, 2011.

[12] S. Kang, "Advanced cooling for power electronics," in *Proc. of International Conference on Integrated Power Electronics Systems (CIPS)*, 2012, pp. 1–8.

[13] J. Schulz-Harder, K. Exel, and A. Meyer, "Direct liquid cooling of power electronics devices," in *Proc. of International Conference on Integrated Power Electronics Systems (CIPS)*, 2006, pp. 1–6.

[14] D. Saums, "Applications of vaporizable dielectric fluid cooling for igbt power semiconductors," in *Proc. of Semiconductor Thermal Measurement and Management Symposium (SEMI-THERM)*, 2011, pp. 253–264.

[15] N. Jankowski, L. Everhart, B. Morgan, B. Geil, and P. McCluskey, "Comparing microchannel technologies to minimize the thermal stack and improve thermal performance in hybrid electric vehicles," in *Proc. of Vehicle Power and Propulsion Conference (VPPC)*, 2007, pp. 124–130.

[16] J. Marcinkowski, "Dual-sided cooling of power semiconductor modules," in *Proc. of International Exhibition and Conference for Power Electronics, Intelligent Motion, Renewable Energy and Energy Management (PCIM)*, 2014, pp. 1–7.

[17] R. C. Burns, "Vertical integration power modules for double sided cooling applications using aluminum conductors and thick film dielectrics," in *Proc. of International Exhibition and Conference for Power Electronics, Intelligent Motion, Renewable Energy and Energy Management (PCIM)*, 2014, pp. 1–8.

[18] C. Buttay, J. Rashid, C. Johnson, P. Ireland, F. Udrea, G. Amaratunga, and R. Malhan, "High performance cooling system for automotive inverters," in *Proc. of European Conference on Power Electronics and Applications (EPE)*, 2007, pp. 1–9.

[19] M. Schneider-Ramelow, T. Baumann, and E. Hoene, "Design and assembly of power semiconductors with double-sided water cooling," in *Proc. of International Conference on Integrated Power Electronics Systems (CIPS)*, 2008, pp. 1–7.

[20] C. Gobl and J. Faltenbacher, "Low temperature sinter technology die attachment for power electronic applications," in *Proc. of International Conference on Integrated Power Electronics Systems (CIPS)*, 2010, pp. 1–5.

[21] J. Kim, "Spray cooling heat transfer: The state of the art," *International Journal of Heat and Fluid Flow*, vol. 28, pp. 753 – 767, 2007.

[22] H. Bostanci, D. Van Ee, B. Saarloos, D. Rini, and L. Chow, "Thermal management of power inverter modules at high fluxes via two-phase spray cooling," *IEEE Transactions on Components, Packaging and Manufacturing Technology,*, vol. 2, pp. 1480–1485, 2012.

[23] D. Bharathan and V. Hassani, "Spray cooling: An assessment for use with automotive power electronics applications," in *National Renewable Energy Laboratory*, 2005.

[24] L. Turek, D. Rini, B. Saarloos, and L. Chow, "Evaporative spray cooling of power electronics using high temperature coolant," in *Proc. of Intersociety Conference onThermal and Thermomechanical Phenomena in Electronic Systems (ITHERM)*, 2008.

[25] R. G. Mertens, L. Chow, K. B. Sundaram, R. B. Cregger, D. Rini, L. Turek, and B. A. Saarloos, "Spray cooling of igbt devices," *Journal of Electronic Packaging. ASME*, 2007.

[26] K. Olesen, F. Osterwald, M. Tonnes, R. Drabek, and R. Eisele, "Direct liquid cooling of power modules in converters for the wind industry," in *Proc. of International Exhibition and Conference for Power Electronics, Intelligent Motion, Renewable Energy and Energy Management (PCIM)*, 2010, pp. 742–747.

[27] A. Bhunia and C.-L. Chen, "Jet impignement cooling of an inverter module in the harsh enviroment of a hybrid vehicle," *Heat Transfer Division and Electronic and Photonic Packaging Division*, vol. 4, pp. 561–567, 2005.

[28] K. Gould, S. Cai, C. Neft, and A. Bhunia, "Liquid jet impingement cooling of a silicon carbide power conversion module for vehicle applications," *IEEE Transactions on Power Electronics*, vol. 30, pp. 2975–2984, 2015.

[29] P. R. Parida, S. V. Ekkad, and K. Ngo, "Impingement-based high performance cooling configurations for automotive power converters," *International Journal of Heat and Mass Transfer*, vol. 55, pp. 834 – 847, 2012.

[30] K. Kellly, T. Abrahan, K. Bennion, D. Bharathan, S. Narumanchi, and M. O'Keefe, "Assessmant of thermal control technologies for cooling electric vehicle power electronics," in *International Electric Vehicle Symposium*, 2007.

[31] C. Barnes and P. Tuma, "Practical considerations relating to immersion cooling of power electronics in traction systems," *IEEE Transactions on Power Electronics*, vol. 25, pp. 2478–2485, 2010.

[32] E. Laloya, . LucÃa, H. Sarnago, and J. M. BurdÃo, "Heat management in power converters: From state of the art to future ultrahigh efficiency systems," *IEEE Transactions on Power Electronics*, vol. 31, pp. 7896–7908, 2016.

[33] I. Mudawar, "Assessment of high-heat-flux thermal management schemes," *IEEE Transactions on Components and Packaging Technologies*, vol. 24, no. 2, pp. 122–141, Jun 2001.

[34] H. Bostanci, D. V. Ee, B. A. Saarloos, D. P. Rini, and L. C. Chow, "Thermal management of power inverter modules at high fluxes via two-phase spray cooling," *IEEE Transactions on Components, Packaging and Manufacturing Technology*, vol. 2, no. 9, pp. 1480–1485, Sept 2012.

[35] M. Lee, J. & Issam, "Two-phase flow in high-heat-flux micro-channel heat sink for refrigeration cooling applications: Part ii, heat transfer characteristics," *International Journal of Heat and Mass Transfer*, vol. 48, pp. 941 – 955, 2005.

[36] ——, "Two-phase flow in high-heat-flux micro-channel heat sink for refrigeration cooling applications: Part i,pressure drop characteristics," *International Journal of Heat and Mass Transfer*, vol. 48, pp. 928 – 940, 2005.

[37] J. Lee and I. Mudawar, "Low-temperature two-phase micro-channel cooling for high-heat-flux thermal management of defense electronics," in *Proc. of Intersociety Conference onThermal and Thermomechanical Phenomena in Electronic Systems (ITHERM)*, 2008, pp. 132–144.

[38] N. Malu, D. Bora, S. Nakanekar, and S. Tonapi, "Thermal management of an igbt module using two-phase cooling," in *Proc. of Intersociety Conference onThermal and Thermomechanical Phenomena in Electronic Systems (ITHERM)*, 2014, pp. 1079–1085.

[39] J. Campbell, L. Tolbert, C. Ayers, B. Ozpineci, and K. Lowe, "Two-phase cooling method using the R134a refrigerant to cool power electronic devices," *IEEE Transactions on Industry Applications*, vol. 43, pp. 648–656, 2007.

[40] K. Lowe, C. Avers, and J. Hsu, "Operating controls and dynamics for floating refrigerant loop for high heat flux electronics," in *Proc. of Semiconductor Thermal Measurement and Management Symposium (SEMI-THERM)*, 2006, pp. 126–129.

[41] G. Moreno, J. Jeffers, S. Narumanchi, and K. Bennion, "Passive two-phase cooling of automotive power electronics," in *Proc. of Semiconductor Thermal Measurement and Management Symposium (SEMI-THERM)*, 2014.

[42] P. Wang, P. McCluskey, and A. Bar-Cohen, "Two-phase liquid cooling for thermal management of igbt power electronic module," *Journal of Electronic Packaging*, vol. 135, 2013.

[43] A. Cavallini, G. Censi, D. D. Col, L. Doretti, G. Longo, and L. Rossetto, "Experimental investigation on condensation heat transfer and pressure

drop of new HFC refrigerants(R134a, R125, R32, R410A, R236ea) in a horizontal smooth tube," *International Journal of Refrigeration*, vol. 24, pp. 73 – 87, 2001.

[44] S. M.R., "Potential refrigerants for power electronics cooling," *Oak Ridge National Laboratory*, 2005.

[45] M. Lazzaroni, M. Citterio, S. Latorre, A. Lanza, P. Cova, N. Delmonte, and F. Giuliani, "Metrological characterization of cold plates for power converters," *IEEE Transactions on Instrumentation and Measurement*, vol. 65, no. 1, pp. 37–45, Jan 2016.

[46] Y. Madhour, J. Olivier, E. Costa-Patry, S. Paredes, B. Michel, and J. Thome, "Flow boiling of r134a in a multi-microchannel heat sink with hotspot heaters for energy-efficient microelectronic cpu cooling applications," *IEEE Transactions on Components, Packaging and Manufacturing Technology*, vol. 1, no. 6, pp. 873–883, June 2011.

[47] C. Park and E. Sunada, "Vapor compression hybrid two-phase loop technology for lunar surfaces applications," in *Proc of CP969, Space Technology and Applications International Forum*, 2009.

[48] L. Yu and D. Liu, "Study of the thermal effectiveness of laminar forced convection of nanofluids for liquid cooling applications," *IEEE Transactions on Components, Packaging and Manufacturing Technology*, vol. 3, pp. 1693–1704, 2013.

[49] H. Lee, L. Song, H. Yunho, R. Reinhard, and C. Ho-Hwan, "Experimental investigations on flow boiling heat transfer in plate heat exchanger at low mass flux condition," *Applied Thermal Engineering*, vol. 61, no. 2, pp. 408 – 415, 2013.

[50] M. A. H. Rasid, A. Ospina, K. E. K. Benkara, and V. Lanfranchi, "A thermal study on small synchronous reluctance machine in automotive cycle," in *Proc. of IEEE 25th International Symposium on Industrial Electronics (ISIE)*, 2016.

[51] S. F. Tie and C. W. Tan, "A review of energy sources and energy management system in electric vehicles," *Renewable and Sustainable Energy Reviews*, vol. 20, pp. 82 – 102, 2013.

[52] P. Beckedahl, T. Grasshoff, and M. Lederer, "A new power module concept for automotive applications." in *Proc. of International Exhibition and Conference for Power Electronics, Intelligent Motion, Renewable Energy and Energy Management (PCIM)*, 2007.